QUANTITATIVE MULTIELEMENT ANALYSIS USING HIGH ENERGY PARTICLE BOMBARDMENT

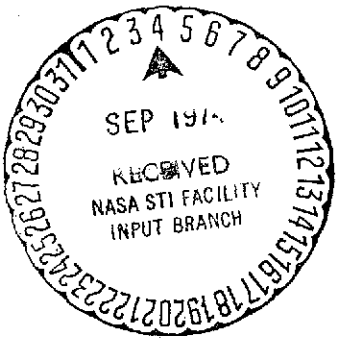

Patrick J. Clark, George F. Neal*, Ralph O. Allen

Department of Chemistry
University of Virginia
Charlottesville, VA 22901

*Present address: Department of Physics, University of Notre Dame, South Bend, Indiana

BRIEF

Water samples and geological materials are analyzed for as many as 28 elements by using 0.8 to 4.0 MeV charged particles to excite X-rays and γ-rays which are monitored simultaneously.

ABSTRACT

Charged particles ranging in energy from 0.8 to 4.0 MeV are used to induce resonant nuclear reactions, Coulomb excitation (γ-rays), and X-ray emission in both thick and thin targets. Quantitative analysis is possible for elements from Li to Pb in complex environmental samples, although the matrix can severely reduce the sensitivity. It is necessary to use a comparator technique for the γ-rays while for X-rays an internal standard can be used. A USGS standard rock is analyzed for a total of 28 elements. Water samples can be analyzed either by nebulizing the sample doped with Cs or Y onto a thin formvar film or by extracting the sample (with or without an internal standard) onto ion exchange resin which is pressed into a pellet.

INTRODUCTION

The possibility of using protons accelerated to energies of several MeV as an excitation source for X-rays or γ-rays has attracted much attention. The bombardment of a target by heavy charged particles frequently results in the ejection of inner shell electrons and the subsequent emission of characteristic X-rays. By using lithium drifted silicon, Si(Li), detectors for energy dispersive analysis, the emitted X-rays can be used for qualitative and quantitative analysis of any element heavier than Na. In a relatively simple sample as little as 10^{-12} gm of an element can be detected (1). In addition to the interaction with electrons, accelerated ions take part in a variety of nuclear scattering and reaction processes. In the MeV energy range, the cross sections for these reactions exhibit sharp resonances associated with the formation of metastable compound systems between the projectile and the target nucleus with a lifetime long compared with typical periods of internal nuclear motion. Protons are especially good for inducing these resonant reactions with light nuclei. By controlling the energy of the bombarding protons it is possible to selectively analyze for one element in a complex matrix because of the narrowness of the resonances. By increasing the energy of the protons above the resonance energy to compensate for the energy loss with penetration depth, this technique has been used as a nuclear microprobe to show depth distribution of the element of interest (2). The γ-rays emitted in these nuclear reactions are characteristic of the compound or product nucleus.

Another type of nuclear excitation is due to the interaction of the Coulomb fields of the projectile and target nuclei, resulting in population of excited nuclear states with subsequent decay by γ-ray emission. The dominant mode of excitation is through the electric quadrupole (E2) interaction (3), thus only nuclei with appropriate low lying nuclear states will be excited in this manner.

Each of the three types of interactions has advantages for analytical applications. The atomic excitation of X-rays is sensitive for elements heavier than Na, but complex matrices can limit sensitivities. Resonant nuclear excitation is selective and sensitive for light elements even in complex samples. The Coulomb excitation gives specific γ-rays for nuclei of each isotope but is much less sensitive. A complete analysis of a target is possible by simultaneously measuring both X-rays and γ-rays. By using the energetically well defined beam from a Van de Graaff accelerator the light elements are measured one at a time in the order of increasing resonance energy. The X-rays are measured at one proton energy. The greatest problem with this type of analysis is in the conversion of integrated peak areas for X-rays and γ-rays to accurate precise elemental concentrations. This paper will describe procedures used for elemental analysis of complex samples such as biological and geological materials by a combination of the proton excitation processes described above.

THEORETICAL

In the bombardment of a target with a charged particle beam, the probability of a nuclear or atomic reaction is expressed as a cross-section which is a function of the kinetic energy of the beam. When the electromagnetic radiation (X-rays and γ-rays) emitted in these reactions is monitored, the yield (Y = events/unit charge) or count rate in a particular detector will depend upon the total cross section ($\sigma(E)$ = cm^2/atom) for formation of the excited state at the bombarding energy E, the product ($k = \prod_f k_f$) of the attenuation factors (k_f) for the emitted radiation or the fraction of excited nuclear or atomic states which result in emission of the radiation being observed, the density of target nuclei (N = particles/cm^3) in the target material, the thickness (X = cm) of the target, the inverse of the ionization charge state of the particles in the beam (I = beam particles/unit charge), the efficiency (ϵ) of the detector for the radiation energy being observed, and the fractional solid angle (Ω) subtended by the detector.

$$dY = NI\Omega\epsilon k\sigma(E)dx \qquad (1)$$

Charged particles readily lose energy in penetrating the target. This energy loss can be expressed as the areal stopping power S(E) which is the rate of energy loss per unit of path length divided by the total target density ($\rho_T = \sum_i \rho_i$ = gm/cm^3 where ρ_i is the partial density of element i in the target).

$$S(E) = \frac{1}{\rho_T}\frac{dE}{dx} \qquad (2)$$

Thus, if the average energy of the particles in the beam impinging on the target is E_o, the energy of the particle in the target is between E_o and the lower average energy (E_f) of the emergent beam which has penetrated the thickness (X) of the target. For a thick enough target the beam is stopped and $E_f = 0$. Since the cross section is a function of the energy, equation 1 must be integrated over the energy range from E_o to E_f. Integrating equation 1 and substituting for $dx = dE/(dE/dx)$ gives:

$$Y = NI\Omega\varepsilon k \int_{E_o}^{E_f} \frac{\sigma(E)dE}{(dE/dx)} \qquad (3)$$

Since $N = \rho i \frac{N_o}{A_i}$ (where N_o = Avogadro's number and A_i = gram atomic weight of element i), using the areal stopping power gives the yield for element i in the target:

$$Y_i = \left(\frac{N_o}{A_i}\right) I\Omega\varepsilon_i k \frac{\rho_i}{\rho_T} \int_{E_o}^{E_f} \frac{\sigma_i(E)dE}{S(E)} \qquad (4)$$

The fraction of the partial densities due to element i ($\rho_i/\rho_T = c_i$) is the concentration of i in the target. In the case of X-ray excitation, the energy resolution obtainable with a Si(Li) detector is not sufficient to measure differences between the isotopes of element i and the elemental concentration c_i can be extracted by measuring the characteristic X-ray yield $\left(Y_i\right)$ according to equation 4.

In the case of nuclear reactions it is necessary to consider the fractional abundance $\left(a_{ij}\right)$ of the jth isotope of element i.

The yield for the particular reaction becomes:

$$Y_{ij} = \left[\frac{N_o}{A_j} \; I \sum_k \epsilon_{ik} \int_{E_o}^{E_f} \frac{\sigma_{ij}(E)dE)}{S(E)} \right] \; c_i \; a_{ij} \qquad (5)$$

A convenient simplification may be introduced where thin targets $\left(\frac{E_o - E_f}{E_o} \ll 1\right)$ are employed. If $|E_o - E_f| = \Delta E$ is sufficiently small such that one may consider $\sigma(E)$ constant over the domain of ΔE, then,

$$\int_{E_o}^{E_f} \frac{\sigma(E)dE}{S(E)} \approx \sigma(\bar{E})T \qquad (6)$$

where $T = \rho_T X$ = areal target thickness, and $\bar{E}$ = the average beam energy at $\frac{X}{2}$.

Quantitative Analysis by Absolute or Comparison Methods

Absolute determination of elemental concentrations requires a good knowledge of the areal target thickness or, in the case of thick targets, the areal stopping power function S(E). For complex matrices, this information is not often easy or even practically possible to obtain. If the target matrix consists of one or two very dominant elements which are known, such that the function S(E) may be considered essentially to be determined by them, then analysis by absolute methods becomes practical. However, this is not necessarily the general case.

Comparison methods consist of three basic types, (a)those where the target sample is doped with a known amount of a known element, (b)those where the concentration of a certain element in a sample is determined by some other method and subsequent measurements of other elements are made relative to it, and (c)"comparator" methods (4) where elemental or isotopic ratios may be determined by reference to a second prepared standard containing the elements or isotopes sought in known relative abundance.

Methods (a) and (b) are identical in principle. Using the subscript R to refer to the reference element or isotope, one may manipulate eq. 5 to obtain:

$$\frac{a_1 c_1}{a_R c_R} = \left(\frac{Y_1}{Y_R}\right) \frac{A_1 \epsilon_R k_R}{A_R \epsilon_1 k_1} \frac{\int_{E_o}^{E_f} \frac{\sigma_R(E)\,dE}{S(E)}}{\int_{E_o}^{E_f} \frac{\sigma_1(E)\,dE}{S(E)}} \qquad (7)$$

If, in addition, a thin target is used, one may employ eq. 6 to arrive at the following:

$$\frac{a_1 c_1}{a_R c_R} = \left(\frac{Y_1}{Y_R}\right) \frac{k_R \epsilon_R A_1 \sigma_R(\bar{E})}{k_1 \epsilon_1 A_R \sigma_1(\bar{E})} \qquad (8)$$

Little additional error is added if E_o is substituted for $\bar{E}$, provided the targets are sufficiently thin. However, for thick samples one still requires a knowledge of S(E), except in certain instances. If, for example, we write $\sigma_1 = B\sigma_R$, where B is a constant with respect to

bombarding energy, then the ratio of integrals in eq. 7 may be replaced by the quantity B^{-1}; this is the case, at least approximately, for certain instances of Coulomb excitation and X-ray production.

A formula for the stopping power (S(E)) proposed by Bethe and later modified by Bloch which is valid for high energies and a single element is given by:

$$S_i(E) = \frac{4\pi e^4 N_o}{M_o c^2 A_i} \quad \frac{Z_b^2 Z_i}{\beta^2} \quad \left[\ln \frac{2M_o c^2 \quad \beta^2}{I \quad 1-\beta^2} \quad -\beta^2 \right] \qquad (9)$$

Here, e = electron charge, M_o = electron mass, c = speed of light in vacuo, N_o = Avogadro's number, A_i = atomic weight of stopping material, Z_i = atomic number of stopping material, Z_b = atomic number of projectile, $\beta = \frac{V_i}{c} = .0463\sqrt{E_i/M_i}$ where E_i is the bombarding particle energy (MeV) and M_i is the particle mass (amu), and I is a quantity related to the ionization potential of the stopping medium and is given by:

$$I \simeq 9.1\ Z_i\ [1 + 1.9\ Z_i^{-2/3}]\ \text{eV} \qquad (10)$$

In principle, the stopping power for a complex matrix can be derived from this, using

$$S(E) = \sum_i c_i S_i(E) \qquad (11)$$

where the c_i are the elemental concentrations (weight percent). Experimentally determined values for $S_i(E)$ have been compiled in a review by Northcliff and Schilling (5).

In the "comparator" methods, it is necessary for the total stopping powers of the unknown and standard target samples to be identical within certain error limits. The samples and standards need not be exactly the same but similar in the relative amounts of major elements as shown by Ricci (4) for biological materials and by Sipple and Glover (6) for sedimentary rocks. Hence, letting primed quantities indicate the standard sample, and recognizing that the same radiation is being observed by the same detector in the same configuration for both the standard and unknown and assuming equality of the stopping powers ($S \approx S'$), then equation 7 becomes:

$$\frac{ac}{a'c'} = \frac{Y}{Y'} \qquad (12)$$

To be completely valid, the beam of charged particles should be completely stopped in both samples; otherwise, the difference in target thickness must be considered.

EXPERIMENTAL

In this work a 5.5 MeV Van de Graaff accelerator is used to produce beams of protons, alphas, or neon ions at well defined energies. Beam currents ranging from 10 nanoamps to about 2 microamps are focused and collimated on the targets. The γ-rays from resonant nuclear reactions and Coulomb excitation are measured using an Ortec Ge(Li) detector. A Kevex Si(Li) detector is used to measure the X-rays from the atomic excitation. Information from each detector is fed through a separate ADC

into one half of the memory of a ND3300 (Nuclear Data) multichannel analyzer. The γ-ray spectrum in one half of the memory and the X-ray spectrum in the other half are read out on magnetic tape for computer analysis on a CDC 6400 at a later date. The experimental arrangement is shown in Fig. 1. During bombardment the target chamber as a whole is electrically insulated to allow integration of the beam current. The Si(Li) detector could be included in the vacuum system or separated by a thin (25.4 μm) Be window. The Si(Li) detector insures good efficiency for X-rays but is insensitive to the higher energy p otons resulting from nuclear reactions. In the case of some γ-rays emitted in reactions the energies are so high that the Ge(Li) detector is not very efficient. In these cases greater sensitivity is possible by using a large volume NaI(Tl) detector since the γ-ray resolution is not very important for the resonant reactions where usually only one type of nuclide is excited.

The simple target holder allows up to 12 samples to be analyzed without breaking the vacuum (and also holds a quartz viewer for beam focussing). Both thick and thin targets are used for a large variety of samples including biological and geological materials. Thick targets are prepared from dry powders by pressing at 3000 psi in a die in a hydraulic press. When there is not enough adhesion, samples are mixed with graphite powder with a Wig-L-Bug (Crescent Dental Mfg.) before pressing. The resulting pellets, which were 1.1 cm in diameter are attached to 1.9 cm Al squares with a small amount of silver conductive paint (manufactured by C.G. Electronics for printed circuit boards) or epoxy and these targets are mounted onto the

sample holder. Thin slices of fine grained rock are also used. Several types of thin targets are prepared by evaporating solutions onto various backings. Drops of solutions placed on Ta or Al disks give non-uniform residues upon evaporation. In order to make the residue uniform, a nebulizer is used to spray the solution onto the backing material. The method described by Jolley and White (7) is used to reduce solid biological and geological samples by ultrasonification to the liquid form, allowing them to be sprayed onto the backing with the nebulizer (DeVilbiss Nebulizer, Model No. 180). In addition to the thick metal backings, thin plastic backings are mounted on an Al washer 1.9 cm in diameter with a center hole 1.1 cm in diameter. The samples are then sprayed onto these thin films of formvar, mylar, polystyrene, or carbon. Commercially available films are greater than 6.35 μm thick but can be made thinner in the laboratory. The advantage of these thin low Z backings is that the background they produce by bremsstrahlung or excitation is negligible.

After a series of samples are placed in the target chamber the energy of the beam is set at the lowest energy of the resonant reaction to be measured and then focused onto a quartz viewer. In succession, each sample is bombarded for a fixed integrated charge without changing the beam and the resulting γ-ray spectra are recorded. Then the beam energy is increased to the next resonance energy and the process repeated for each sample. At the highest resonance energy the X-ray spectra are recorded along with the γ-ray spectra.

RESULTS AND DISCUSSION

"X-ray Excitation"

The main advantage of using heavy charged particles for X-ray excitation is that the background can be quite low while the cross section for X-ray production remains high. The background associated with the heavy ion is bremsstrahlung caused by the secondary electrons. Classically the maximum energy imparted to an electron in a head on collision can be calculated as four times the product of the ratio of electron to ion mass and the energy of the ion. Thus a 4 MeV alpha particle, which can excite X-rays above 20 keV, produces electrons with less than 2 keV of energy, keeping the bremsstrahlung background confined to low energies. This can be compared to using electron excitation where the bremsstrahlung covers the entire energy region being excited or excitation with monochromatic X-rays which because of Compton scattering has the highest background just below the energy of the exciting line. Cairns (8) sites an improvement in the peak/background ratio of from 10^3 for 20 keV electrons to 10^5 for 2 MeV proton excitation with comparable X-ray yields. The lower energy of the background for heavy ion excitation can be easily suppressed by simple filters (8). However, the use of absorbers adds complications to accurate quantitative analysis. When thin targets are used, the background is, of course, much smaller than for thick targets.

Figure 2 compares the X-ray spectrum for proton excitation on a thick graphite-containing target (a) and a thin film of formvar (b). In both cases the sample is the USGS standard rock BCR-1. In (a) 0.1984 gm of the rock is mixed with 10% graphite powder (National Spectroscopic grade SP-1C) which acts as a binder and also provides electrical conduction, before being pressed into a pellet. In the thin sample (b) 0.002 gm of BCR-1 is nebulized onto a 100 μg/cm^2 thick formvar film. Proton current on the sample is limited to 25-30 nA, and a total of 40 micro-Coulombs of charge is collected, since only the major elements are sought. Note the difference in the 3 to 5 keV region under the X-ray peaks for K, Ca, Ti and V. A 20 mg/cm^2 Al absorber is placed between the thick sample (a) and the Si(Li) detector to decrease the total count rate by eliminating some of the low energy bremsstrahlung.

Several types of thin targets are prepared from formvar (100 μgm/cm^2), mylar (640 μg/cm^2), and polyvinylidene chloride (1200 μgm/cm^2) and analyzed for background. In all of these materials the largest amount of background is in the low energy (2-3 keV) bremsstrahlung region. The intensity of the background increases with increasing target thickness. Obviously the characteristic Cl X-rays in polyvinylidene chloride make it undesireable. The formvar is superior to the mylar because of its higher heat resistance allowing use of higher currents (up to 100 nA with no cooling). The formvar films prepared in this laboratory are thinner than the commercial mylar used which means that the background is nearly two orders of magnitude lower for the formvar. The one advantage of mylar is that the position of the beam on the

target could be observed due to the fluorescence in the mylar. For both the thin hydrocarbon backings and the thick graphite-containing pellets an additional source of low energy background is from the periodic discharge which occurs when a positive charge builds up on the nonconducting targets. This is a significant source of background in the thin target experiments but it can be largely eliminated by placing a bare filament in the target chamber to spray thermal electrons onto the target, thus preventing positive charge accumulation (9). This background source is eliminated from the thick graphite-containing targets by attaching them to the Al backing with the conducting silver paint rather than the epoxy. It is not possible to assign absolute values to the sensitivity obtainable by this technique as it depends upon the experimental arrangements, e.g. the detector solid angle and other characteristics. However, the relative sensitivities can be quite well described by the production cross section (the ionization cross section times the fluorescence yield).

Experimental measurements (10, 11) of cross sections suggest that the binary encounter approximation (BEA) predicts the ionization cross sections very closely. The fluorescence yields have been compiled by Bambynek et al. (12). Figure 3 shows the ionization cross sections for the three types of particles used in this study (H^+, He^+, Ne^+) as a function of the atomic number of the target. These measurements were made using the University of Virginia 5.5 MeV Van de Graaff accelerator (10). In general this indicates that protons

are the best particles for excitation because for a given particle energy the ionization cross sections are greater by at least an order of magnitude. However, in complex samples there may be a problem with too many X-rays excited for the detector to function well. In this case the heavier particles (like neon) are more selective in that elements within rather limited ranges of atomic numbers are efficiently excited. In addition Cairns (8) has pointed out that below a certain critical energy a bombarding heavy ion will not excite X-rays. Thus, by careful choice of heavy bombarding ion and energy, a particular element can be selectively excited. For a more complete characterization of the sample, however, the protons are more universal. In addition to the cross sections, the background differences and depth of penetration must also be considered. The bremsstrahlung background is at lower energies and the depth of penetration is much lower for the heavier particles.

An absolute measure of the sensitivity is determined by nebulizing and evaporating 10 ml of a dilute aqueous solution onto a formvar film and measuring the yield. Table 1 indicates these sensitivities obtained by extrapolating the peak area obtained down to a value of twice the uncertainty in the background obtained from the same integrated charge ($1000\mu C$) on a blank formvar film. These calculations are based on a solid angle of 5.5×10^{-4} steradians subtended by the Si(Li) detector. Another method of analyzing for trace elements in aqueous solutions is to extract onto an ion exchange resin which can be pressed into a pellet (using 10% graphite). Table I also gives the sensitivities obtained by

extracting 10 ml of the same solutions as used for the thin films onto 0.250 gms Bio-Rad Chelex 100 resin. The advantage of this technique is that larger liquid volumes could be rapidly batch extracted onto the resin, thus improving the sensitivity.

The greater sensitivity obtained by using the ion exchange resin also is due to problems with the nebulization technique. The spray covers a larger area than the resin pellet, but the size of the proton beam is constant. Therefore, a smaller fraction of the evaporated target is sampled. In addition, our experiments have indicated that there is also substantial loss of the material in solution due to deposition inside the nebulizer. The pellets give a uniform and reproducible target 1.1 cm in diameter. In contrast the sample on the thin film, limited by the Al washer to the same size, is not uniformly distributed and hence is less reproducible. Thus in terms of both time required and greater sensitivity, the resin technique is best for routine water analysis. For more complex samples such as geological materials, analysis is more difficult and less sensitive. This is due to the high intensity of the K X-rays for the relatively light major elements. These obscure the low intensity L X-rays in the same region, cause pulse pile up in the electronic circuitry, and degrade the resolution.

Two methods of quantifying the analysis of aqueous solutions are investigated. In the comparator method a standard solution is used to prepare a target containing the elements of interest. The X-ray intensities from the sample can be compared directly with those from the standard. This does require that conditions be kept uniform for the sample and standard. For instance, the targets must be uniform and reproducible and either the areal density or total weight of the sample must be known. The non-uniformity of the thin film targets prepared by nebulizing and evaporating makes precision impossible using the comparator technique. The only precise way to analyze the thin targets onto which aqueous solutions have been nebulized is to use an internal standard technique. In the case of the resin pellets the precision is very good. Individual pellets, each containing Cs and three other elements which were extracted from 1 ml of solution, are prepared. Another pellet is prepared by extracting from a mixture of the nine elements. This pellet is used as a standard to calculate the concentrations in the other resin pellets. Table II shows the results of using the comparator method for solutions extracted onto the resin. The accuracy is good (within expected uncertainties in counting statistics) except in cases where selective absorption and enhancement effects occurred in the standard mixture (not shown). The necessary corrections for this type of effect can be made using techniques such as those described by Rasberry and Heindrich (13).

By knowing the production cross sections, the mass absorption coefficients, and the thickness of any absorbers between the sample and detector, absolute concentrations can be determined by comparing the intensity of the X-rays from each element to an element which has been added to the original solution at a known concentration. Gove et al. (14) suggests $CsNO_3$ as the doping material since it is soluble and the ions do not form precipitates. Both the 4.29 keV $L\alpha$ and 30.8 keV $K\alpha$ X-rays can be used. In this work, and Gove's (14), the cesium concentrations are varied (100-1000 ppm) to ensure that the results were independent of the dopant concentration. The standard solution used for the comparator method is doped with Cs and the concentrations measured by the internal standard method are shown in Table II. In this case 5 ml of the doped solution is nebulized onto the formvar backing. Relatively poor precision and accuracy can result from the high background (due to the charge buildup on the target) under the Cs L X-ray. The background could be eliminated with thermal electrons (9) or could be avoided by using Yittrium as the internal standard for Y. The X-ray energies are $K\alpha$ (14.93) and $L\alpha$ (1.92). and it is not a common contaminant in water samples, is soluble as the nitrate, and does not interfere with any of the other elements which might be sought in environmental samples. The resin samples could also be analyzed by this internal standard technique. The results for the mixture of nine elements is also shown in Table II. It should be noted that the uncertainties are higher for the internal standard results than for the comparator results due to the uncertainties in production cross sections. Again corrections for selective enhancement and absorption in the thick samples are necessary.

"Nuclear Resonant Reactions"

The nuclear reactions used are either inelastic proton scattering with subsequent γ-ray emission $(p,p'\gamma)$ or proton absorption followed by emission of an alpha particle and/or decay to the ground state $(p,\alpha\gamma)$, (p,γ). The cross sections for these reactions vary with energy, being small except for narrow energy bands or resonances where they are as much as several orders of magnitude higher. The energies and widths of the resonances may be found in the nuclear physics literature. One example is shown in Fig. 4 for three ^{27}Al (p,γ) ^{28}Si resonances. A thin Al film ($\sim 100\ \mu g/cm^2$) is vacuum deposited on a 0.25 mm Ta backing. The energy of the protons bombarding the target is increased in steps of 2 keV and the counts for 300 micro-Coulombs of integrated charge are recorded. Note the slight tailing of the peaks on the high energy side due to the finite thickness of the Al layer. In fact, since the rate of energy loss for the proton $\left(\frac{dE}{dx}\right)$ can be calculated, it is possible to use these resonant reactions as a measurement of depth (2). For instance, deposition of another layer of material (other than Al) on the Al surface changes Figure 4 by shifting the peak up on the energy scale to a degree which depends on the thickness of the covering layer.

At the resonance energies the reactions listed in Table III are selective in the sense that only one reaction is prevalent, however, at higher energies (especially for thick samples) other reactions

also occur. The reactions used must be chosen to yield unique products (a unique γ-ray spectrum) to avoid interferences between different nuclear reactions yielding the same final isotope. The unique γ-ray spectra of the products and the enhanced cross sections at resonance energies combine to make this a very selective technique. Sensitivities are measured using thick target pellets formed from USGS standard rocks mixed with graphite. Thin targets are prepared by nebulizing solution onto thin formvar films, but the resulting non-uniform target does not allow the necessary precision. Vacuum deposition is used to put a uniform thin layer of the desired element on a Ta backing (as in Fig. 4). The minimum detectable limit is defined as a γ-ray peak (minus background) larger than two standard deviations of the background in that region of the spectrum. The results are tabulated in Table III.

In the case of the thin films the thickness is known so that sensitivities can be calculated in units of mg/cm^2. If the area covered by the beam is known (in this case measured to be approximately 0.07 cm^2) sensitivity can be calculated in terms of grams on the surface of the target. When the proton beam is set at the resonance energy the thickness of material sampled is very small and depends upon the width of the resonance. Thus, in the case of the thick geological samples, the sensitivities (in ppm) may appear poorer because such a small portion of the sample is actually being analyzed.

For quantitative analysis the comparator method must be used. Since Van de Graaff accelerators can be held at a particular energy a series of samples should be analyzed for a single element before going to the proton energy required for the next element. The only critical factor, besides the energy, which must be kept constant is the angle of the sample relative to the beam and the γ-ray detector. It should be noted that this nuclear microprobe technique can be used to measure spatial distribution with a well focussed beam (15) or to measure the average concentration using a defocussed beam as was used in this work.

"Coulomb Excitation"

The excitation of the nucleus by the interaction of its Coulomb field with that of the bombarding nucleus is a purely electromagnetic process. The cross section for Coulomb excitation depends on several factors including the energy, spin and parity of the excited nuclear state being populated relative to the ground state, the energy of the bombarding particle, and the strength of the Coulomb interaction. The last is described by the Sommerfeld number $\xi = \frac{Z_p Z_t e^2}{hV}$ (Z_p and Z_t are the nuclear charges on the projectile and target nuclei respectively and V is the velocity of the bombarding particle). The classical treatment of this phenomena (3) indicates that unless $\xi \geq 4$ use of this excitation for analysis would not be practical. This relationship means that Coulomb

excitation is more probable for targets with high atomic numbers and for the heavier alpha bombarding particles. This, however, does not take into account the fact that the nucleus must have a low lying excited state. As the energy of this excited state increases, the excitation probability decreases, but at different rates for protons and for alphas. The ratio of the cross sections using 4 MeV protons versus 4 MeV alphas is calculated as a function of the excitation energy for four different values of Z_t and plotted in Figure 5. Thus, the decision as to the best type of bombarding particle must be made with respect to the energy level being excited. It should be kept in mind that the proton has a greater range in a thick target and, therefore, samples a larger volume. However, even under the most favorable circumstances the cross sections for these reactions are low.

In Table IV the sensitivities for a few of the most favorable isotopes are given. These are measured by analysis of thin films of the elements vacuum deposited on Ta backings. Again the vacuum deposition is used because the nebulized aqueous solution is not as uniform. In addition the Ta backing allowed greater beam currents and thus more rapid data collection. The limit of 0.1 counts/μ Coulomb for a Ge(Li) detector 10 cm from the target is set on the basis of the low background for these samples (except for Ta peaks). In more complex samples, such as geological materials (Fig. 6), the background is higher due to the increased Compton scattering of the γ-rays produced

by some of the resonant nuclear reactions listed in Table III. This increased background decreases the sensitivity by as much as two orders of magnitude.

If the Coulomb excited γ-rays are used to analyze samples, a comparator technique is necessary. Although the sensitivities are not very good, this phenomenon is quite selective and so could be of use for particular applications such as measuring one of the elements in Table IV in a matrix which does not yield Coulomb excited γ-rays. In this work it is found that some of these elements could be measured in samples at the same time as the X-rays and the γ-rays from the nuclear resonant reactions. Thus, while perhaps not a valuable analytical technique by itself, when combined with the other two types of excitation it can provide useful information.

Analysis of Geological Materials

For solid materials, e.g. rocks or lyophilized biological samples, the best sensitivity is obtained by forming a pellet using 10% graphite. These samples can withstand larger beam currents than the thin films although the thick target makes it necessary to correct for the loss in energy of the bombarding particle as it passes through the sample. The stopping power of a thick sample can be considered as a matrix effect since different volumes of material are sampled. If the internal standard method is used, then the only matrix effect which need be considered is the differential absorption of X-rays of different energies which can be

taken into account using programs such as those described by Brown et al. (16). In order to use the comparator method the mass stopping power $(1/\rho)(dE/dx)$ must be known. Since most geological materials are composed of a few major elements in a narrow range of atomic numbers, the stopping powers do not vary appreciable between different samples. Table V gives the values of $(1/\rho)(dE/dx)$ for five different proton energies in a number of USGS rock standards (17) calculated using the data of Northcliff and Schilling (5). Although these igneous and metamorphic rocks cover a wide range of compositions, the stopping powers for a particular energy are very similar. For each energy the average and the deviation from the mean are given. This indicates that by using one of these standardized rock powders for comparison, almost any type of rock can be analyzed without a correction for the small differences in stopping powers. It should be pointed out that the volume of specimen actually sampled is small since the depth sampled depends upon the range of the bombarding particle. The proton beam used for analysis is on the order of 3 mm in diameter and the actual amount of rock pellet being sampled by a 4 MeV proton is calculated (5) to be on the order of 3.5×10^{-3} gms. Therefore, unless the sample is carefully powdered and mixed, sample inhomogenieties may lead to imprecise results. In the case of the nuclear resonant reactions an even smaller amount of specimen is effectively sampled, the actual depth depending upon the width of the resonance.

The proton resonance and X-ray analysis of replicate samples of the same USGS standard are reproducible within the uncertainties due to counting statistics. The most critical factor is found to be controlling the angle of the target relative to the beam and detector. The necessary precision should be built into the sample holder.

In order to show the potential of a combination of the three techniques described above, several USGS standard rocks are analyzed. A granite (G-2) is used as the primary standard and the concentrations are calculated by comparison. The results of one of these rocks (a basalt, BCR-1) are given in Table VI along with the range of values reported by Flanagan (17). Some of the deviations from the best values reported for BCR-1 may be due to sample inhomogenieties on the macro or micro scale and some (such as for Li) are thought to be partially due to problems in proper positioning of the sample. The data for the other rocks is as good, but not as complete, as the BCR-1 results.

The analysis sequence for a set of samples such as these geological standards is as follows: 1)prepare pellets using ~10% graphite as binder, 2)mount samples with silver conductive paint onto Al squares, 3)align the samples on the holder and mount in sample chamber, 4)after evacuating the chamber set proton energy at 0.991 MeV(^{19}F resonance) and focus the beam on the quartz window, 5)irradiate the standard (G-2) with 0.5μamps and count the γ-rays for 1,000μCoulombs or until adequate counts are obtained (as long as the collected charge is measured),

6)store γ-ray spectrum on magnetic tape and move the first sample into the beam, 7)repeat data collection for each sample at a particular energy and then change to energy of next resonant reaction and analyze the standard and each sample, 8)after finishing the P resonance at 3.73 MeV increase proton energy to 4.0 MeV and collect both X-ray and γ-ray spectra for 50 μCoulombs. An example of the X-ray spectra is that for BCR-1 shown in Figure 2a. The γ-ray spectrum for BCR-1 obtained at the same time is shown in Figure 6.

The photopeaks in the γ-ray spectra taken at 4 MeV are due mostly to nuclear reactions. Since the target is thick at different depths within the sample the proton has lost enough energy so that it is at one of the resonance energies for each reaction. The intensities of these peaks are used to calculate the concentrations of the different elements and the results agree with those taken earlier for the analysis of the surface. This indicates that the samples are homogeneous. In addition to these large photopeaks there are several peaks due to Coulomb excitation. The peaks observed are noted in Table VI along with the calculated concentrations using G-2 as the standard. The lack of sensitivity is readily apparent. The concentrations obtained for the light elements using the nuclear resonant reactions are also given.

In the case of the X-rays, corrections are made for absorption and secondary fluorescence by some technique such as that of Brown et al. (16).

This type of correction requires the analysis of more than one standard to initially calculate intensity ratios. Once these are calculated a single standard can be used as a monitor for each set of unknown samples. The sensitivity could be improved by longer counting and irradiation times.

Use of the energy dispersive Si(Li) detector for the analysis of complex samples suffers from the lack of resolution. A detector with higher resolution than that used for this work would eliminate some of the overlap of peaks. In order to reduce the resolution problem a deconvolution program was written for the CDC 6400. This program fits the background region of the spectrum with an exponential or power series polynomial and subtracts the fit from the spectrum. The spectrum with background subtracted is examined for photopeaks using the standard deviation above background and numerical first and second derivatives at each data point as criteria. Multiplets found from the maxima and minima of the second derivative are resolved with the option of fitting each multiplet to a function consisting of N gaussians. The program provides peak limits, centroid, and area for each resolved peak.

The analysis of these geological samples is an indication of the possibilities for analyzing complex samples. A total of 28 elements are measured simultaneously. With longer irradiations and a better Si(Li) detector more elements could be measured. The greatest sensitivities are, however, obtained by analyzing solutions nebulized and evaporated onto thin formvar films or extracted onto ion exchange resin which is formed into a pellet. As discussed above, the X-ray

intensities can be converted to concentrations using the internal standard or comparator method. The γ-rays from resonant reactions or Coulomb excitation can be measured at the same time as the X-rays, but quantitative analysis requires a standard containing the elements of interest for comparison. Preparation of thin uniform targets and the limitations in beam current are problems. This is a very sensitive technique for environmental studies or liquid samples. Although a large particle accelerator is necessary for this type of analysis, time on these machines is becoming increasingly available for analytical work. The calculations can be more straightforward than for neutron activation analysis if the samples are prepared as described above so that the rather complex equation 5 can be simplified.

ACKNOWLEDGEMENTS

The authors gratefully acknowledge the financial support provided by the National Aeronautics and Space Administration (NGR-47-005-176) and the technical support provided by the University of Virginia Department of Physics.

TABLE I. Detection Limits for 4.0 MeV Charged Particle-Induced X-rays[a]

Element		FORMVAR Protons (10^{-9} gm)	FORMVAR Alphas (10^{-9} gm)	RESIN Protons (10^{-9} gm)
Cl	K_α	12.2	--	1.40
Co	K_α	5.9	7.6	0.81
Ni	K_α	8.3	11.2	1.18
Ge	K_α	15.2	72.5	1.33
Se	K_α	46.8	75.0	1.67
Rb	K_α	52.1	246.0	2.11
Cd	K_α	165	--	9.13
Cs	K_α	--	--	79.5
Tl	L_α	42.3	109	3.33

[a] Limits defined for the minimum detected by nebulizing (for formvar) or extracting (for resin) 10 ml of solution and measuring X-rays for 1,000 μCoulombs of integrated charge.

TABLE II. Determination of Elemental Concentrations Using 4.0 MeV Proton-Induced X-rays

Element	Cesium Internal Standard[a]		Comparator Method[b]	Actual, ppm
	Formvar Backing, ppm	Ion Exchange Resin, ppm	Ion Exchange Resin, ppm	
Cl	17.6 ± 2.5	16.2 ± 2.4	--	16.3
Co	27.4 ± 3.6	27.6 ± 3.6	25.9 ± 0.2	25.3
Ni	31.1 ± 4.0	26.8 ± 3.4	25.3 ± 0.3	27.0
Ge	24.6 ± 3.0	22.8 ± 2.8	--	25.6
Se	26.9 ± 3.2	26.8 ± 3.1	23.1 ± 0.2	25.8
Rb	30.7 ± 3.8	27.6 ± 3.2	--	24.7
Cd	29.9 ± 3.9	22.6 ± 2.5	24.9 ± 1.8	26.0
Cs	--	--	232 ± 17	250
Tl	25.1 ± 2.0	26.1 ± 2.1	--	25.8

[a] Solutions doped with 250 ppm Cesium.

[b] Mixture of all nine elements used as the standard.

TABLE III. Detection Limits for Resonant Nuclear Reactions[a]

Reaction	Proton Energy (MeV)	Gamma Energy (MeV)	Thin target[b] Limit, μgm	Thick target[c] Limit, ppm
$^{7}Li\ (p,\ p'\gamma)^{7}Li$	1.030	0.478	0.10	0.69
$^{9}Be(p,\gamma)^{10}B$	0.991	7.50	--	--
$^{10}B(p,\gamma)^{11}C$	1.532	0.429	0.84	<2200
$^{11}B(p,\ p'\gamma)^{11}B$	2.664	2.144	0.70	<2000
$^{12}C(p,\gamma)^{13}N$	1.700	3.51	--	--
$^{15}N(p,\alpha\gamma)^{12}C$	0.898	4.430	--	--
$^{19}F(p,\ \alpha\gamma)^{16}O$	1.375	6.130, 7.120	1.3	0.96
$^{23}Na(p,\ p'\gamma)^{23}Na$	1.458	0.439	0.024	0.58
$^{24}Mg(p,p'\gamma)^{24}Mg$	2.930	1.370	--	28.7
$^{27}Al(p,p'\gamma)^{27}Al$	2.727	1.013	--	23.3
$^{28}Si(p,p'\gamma)^{28}Si$	3.100	1.779	510	62.3
$^{31}P(p,p'\gamma)^{31}P$	3.730	1.266	12.0	1.1
$^{32}S(p,p'\gamma)^{32}S$	3.379	2.237	1.8	3.5
$^{35}Cl(p,p'\gamma)^{35}Cl$	2.721	1.220, 1.763	2.1	6.2

[a] Based on 1000 μCoulombs of integrated charge.

[b] Thin target (100 $\mu g/cm^2$) prepared by vacuum deposition of material onto 0.25 mm thick Ta backing.

[c] Thick targets (1 mm) were prepared by pressing a mixture of rock powder and 10% graphite.

TABLE IV. Detection Limits for 4.0 MeV Charged Particle-Induced Coulomb Excitation Gamma Rays[a]

Element	Isotopic Abundance	Gamma Energy, keV	Minimum detectable Weight for Thin Target, μg		Minimum detectable Concentration in Thick Target, mg/gm	
			proton	alpha	proton	alpha
^{47}Ti	7.3	159	0.48	0.15	0.2	0.7
^{48}Ti	73.9	983	0.44	6.30	0.2	30.0
^{55}Mn	100	126	0.03	0.01	0.01	0.04
^{56}Fe	91.7	847	0.32	3.78	0.1	18.0
^{57}Fe	2.2	136	2.17	0.68	1.0	3.2
^{75}As	100	199	0.26	0.10	0.002	0.5
^{77}Se	7.6	239	0.77	0.38	0.3	1.8
^{80}Se	49.8	666	0.46	4.13	0.2	19.7
^{181}Ta	100	136	0.08	0.04	0.03	0.2
^{181}Ta	100	301	0.48	2.24	0.01	10.7
^{197}Au	100	192	2.52	3.22	1.2	15.3
^{197}Au	100	279	0.51	2.31	0.2	11.0

[a] Based on 0.1 cts/μCoulomb detected in Ge(Li) 10 cm from target.

TABLE V. Stopping Powers for USGS Rock Standards[a]

Proton Energy, MeV	USGS STANDARD G-2	PCC-1	GSP-1	BCR-1	G-1
1.0	194.76	194.95	193.71	189.49	194.94
2.0	119.40	119.41	118.89	116.75	119.50
3.0	89.04	89.05	88.71	87.29	89.11
4.0	71.80	71.81	71.56	70.50	71.85
5.0	60.72	60.73	60.53	59.68	60.77

Proton Energy, MeV	DTS-1	AGV-1	W-1	Average	Standard Deviation
1.0	195.25	192.66	190.13	193.24	2.28
2.0	119.56	118.35	117.09	118.62	1.13
3.0	89.14	88.35	87.52	88.53	0.74
4.0	71.88	71.29	70.67	71.42	0.55
5.0	60.79	60.31	59.82	60.42	0.44

[a]Stopping powers in units of keV·cm^2/mg, based on major element compositions (17).

TABLE VI. Measurement of Elemental Concentrations in Geological Standard BCR-1[a]

Element	Reported[b], ppm	Proton Resonance, ppm	X-ray Excitation, ppm	Coulomb Excitation, ppm
Li	12.8	12.4 ± 0.8	--	--
F	485	491 ± 9	--	--
Na	2.42%	2.46 ± 0.03 %	--	--
Mg	2.08%	2.06 ± 0.04 %	--	--
Al	7.20%	7.12 ± 0.2 %	--	--
Si	23.82%	23.8 ± 0.3 %	--	--
P	0.157%	0.140 ± 0.03 %	--	--
S	392	384 ± 10	--	--
Cl	50	43.2 ± 2.5	--	--
K	1.41%	--	1.10 ± 0.52 %	--
Ca	4.94%	--	4.37 ± 0.30 %	--
Ti	1.27%	--	1.24 ± 0.02 %	1.13 ± 0.28 %
V	399	--	390 ± 4	334 ± 72
Cr	17.6	--	18.5 ± 0.5	--
Mn	1406	--	1390 ± 12	1238 ± 240
Fe	9.37%	--	9.14 ± 0.02 %	8.46 ± 1.52 %
Cu	18.4	--	17.7 ± 0.6	--
Zn	120	--	118 ± 2	106 ± 28
Ga	20	--	19.5 ± 2.2	--
As	0.70	--	0.70 ± 0.02	--
Rb	46.6	--	45.2 ± 1.2	--
Sr	330	--	332 ± 0.4	--
Y	37.1	--	38.2 ± 2.1	--
Zr	190	--	188 ± 2.4	--
Nb	13.5	--	15.4 ± 2.0	--
Ag	0.036	--	0.032 ± 0.003	--
Sb	0.69	--	0.66 ± 0.06	--
Ba	675	--	705 ± 48	--

[a] Using G-2 as a standard.

[b] Best values given by Flanagan (17).

REFERENCES

1. T. B. Johansson, R. Akselsson, S. A. E. Johansson, Nucl. Instrum. Methods, 84, 141 (1970).

2. D. A. Leich and T. A. Tombrello, Nucl. Instrum. Methods, 108, 67 (1973).

3. K. Alder and A. Winther, Eds., "Coulomb Excitation", Academic Press, Inc., New York, 1966.

4. E. Ricci, Nucl. Instrum. Methods, 94, 565 (1971).

5. L. C. Northcliffe and R. F. Schilling, Nucl. Data Tables, A7, 233 (1970).

6. R. F. Sippel and E. D. Glover, Nucl. Instrum. Methods, 9, 37 (1960).

7. R. K. Jolly and H. B. White, Jr., Nucl. Instrum. Methods, 97, 103 (1971).

8. J. A. Cairns, Nucl. Instrum. Methods, 92, 507 (1971).

9. B. K. Barnes, L. E. Beghian, G. H. R. Kegel, S. C. Mathur and P. W. Quinn, Meeting of the American Physical Society, Washington, D. C., April, 1973, No. EO 13.

10. R. McKnight, Phys. Rev. (1974), In Press.

11. T. J. Gray, North Texas State University, Denton, Texas, Personal Communication, 1973.

12. W. Bambynek and B. Crassemann, Rev. Mod. Phys., 44, 716 (1972).

13. S. D. Rasberry and K. H. F. Heinrich, Anal. Chem., 46, 81 (1974).

14. H. E. Gove, D. Stupin, A. Pape, A. Gallman, G. Guillaume, P. Fintz, and J. C. Sens, Division of Nuclear Physics, Seattle, Washington, November, 1972.

15. T. B. Pierce, P. F. Peck and D. R. A. Cuff, Nucl. Instrum. Methods, 67, 1 (1969).

16. G. E. Brown, D. J. Hughes and J. Esson, Chem. Geol., 11, 223 (1973).

17. F. J. Flanagan, Geochim. Cosmochim. Acta, 33, 1189 (1973).

FIGURE CAPTIONS

Figure 1. Schematic diagram of target chamber and detection system.

(A)vacuum fitting to allow target holder adjustment, (see enlargement inset),

(B)target mounted on Aluminum holder,

(C)quartz disc for focussing particle beam,

(D)reference scale for sample positioning,

(E)facuum fitting for Si(Li) detector connection to target chamber, o-rings indicated by solid circles, (see enlargement inset),

(F)beam stop.

Figure 2. Characteristic X-ray spectra for USGS BCR-1 as a)10% graphite pellet and b)deposited on formvar film.

Figure 3. Ionization cross sections for K and L X-ray production by 4 MeV heavy charged particles.

Figure 4. Gamma-yield for the $^{27}Al\ (p, \gamma)\ ^{28}Si$ reaction.

Figure 5. Ratio of the Coulomb excitation cross sections for 4 MeV protons to alphas as a function of nucleus excitation level.

Figure 6. Characteristic gamma-ray spectrum for USGS BCR-1.